

Names: Carina Grady, Courtney Smyth

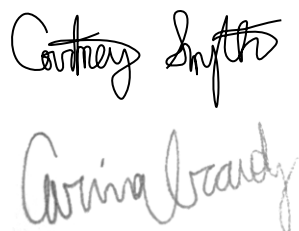
Lab Section: 5

Laboratory Number: 5

Laboratory Title: CFD

I attest that the attached laboratory report represents my own original work. The data presented was collected by my lab partners and myself, and the lab report was written by myself. I understand that if the attached report is found to contain data other than those collected by my lab partners and myself, or if the attached report is found not to be my own original writing, the penalty will be zero on the report and a full letter grade reduction on my final lab grade.

Signed:



The image shows two handwritten signatures in black ink. The top signature is 'Courtney Smyth' and the bottom signature is 'Carina Grady'. Both are written in a cursive, flowing style.

## 1. Abstract

The purpose of this lab was to do mesh-convergence analysis on a computational fluid dynamics program, ANSYS, which aimed to determine if the amount of elements in the domain influenced the output solution. Along with this, the distributions for velocity and pressure within the domain were analyzed for different flow rates. Nine simulations were run using a coarse, medium, or fine mesh, as well as a Reynolds Number of 50, 100, or 150. Fluid was run through a two inch diameter tube, with an obstruction at the halfway point. It was found that there was a point at which the output was independent of the number of elements used, however, even the coarse mesh had already exceeded the cutoff. This produced a graph that was close to level for each of the three Reynolds Numbers. It was also found that the velocity and pressure distributions within the domain were different depending on the Reynolds Number used. For the largest Reynolds Number (also the largest flow rate), the velocity was higher for a larger amount of time after the obstruction was passed. This occurred in all three of the mesh refinements. The pressure contours showed that there was negative pressure occurring around the obstructions for the higher flow rate cases, as well. The overall conclusion was that mesh refinement was important for a more accurate solution up until a certain point, and that the higher flow rates caused a larger impact on velocity and pressure around the obstruction.

## 2. Introduction

Computational Fluid Dynamics (CFD) is an important method for simulating and determining solutions to complex fluid mechanics problems. Computers use numerical methods to analyze and solve these problems. Common fluid flow software includes: ANSYS Fluent, Comsol, CFX, KIVA, Star-CD, and OpenFOAM. While this lab focused on Fluent, each has its own advantages and disadvantages that industries can use to best utilize certain features. There are a myriad of industries in which CFD is an important tool in. Examples are the aerospace industry, where airflow is a focus; the automotive industry, where drag forces along the car front plays a large role; the HVAC industry, where air flow/ distribution is important for temperature control in spaces; and many more. The user can input data or environment conditions, as well as create a specific geometry he/she is interested in studying. Once the inputs are entered, the computer processes through running a series of iterations that continue to produce more and more accurate solutions. Once the simulation is run, there are many visual plots, diagrams, and graphs available to boil down trends and data into user friendly outputs [1].

Another advantage of using CFD in industry is the speed at which computations can be done, as well as the option to set a desired error. This is a large benefit, because applications that require a very small error can run programs, such as Flunt, until the output numerical solution converges to an error smaller than what is necessary. This ensure results that are accurate to the degree that is needed, and the program will not converge if the desired error is smaller than is possible. As mentioned previously, CFD is an extremely important tool in many engineering industries, and makes solving seemingly impossible problems possible. This lab aimed to determine if the output solutions of water flowing laminarly through a tube were dependent on the mesh refinement, as

well as how the distributions of velocity and pressure differed along the obstruction due to a change in the flow speed [2].

### 3. Theory and Experimental Methods

As noted previously, using CFD would tremendously aid in reducing the time needed to compute the results compared to meticulously calculating the answers by hand. Because industry uses CFD software like ANSYS, the objective of this lab was to use ANSYS and analyze if the results depend on how fine the mesh is. The following variables are tested: a laminar Reynolds Number of 50, 100, and 150; and a mesh size of coarse, medium, and fine. This results in nine data sets. With each data set, the following results are obtained from a pipe and then compared: total drag force on the orifice-plate, axial velocity and pressure at every point of the horizontal pipe, static pressure along center line, and plot of axial velocity profile vs. radial distance along the outlet.

Since ANSYS automatically calculates everything, only one equation was needed to correctly set-up the lab. Although Reynolds number (Re) was given, velocity was not, and velocity was a necessary input to run the simulation. Equation [1] below denotes the equation that relates Re with velocity. Refer to Appendix C for a sample calculation.

$$Re = \frac{\rho v D}{\mu} \quad \text{Equation [1]}$$

After computing the three different velocities for the three different Reynolds Numbers, all that was left was to correctly set up ANSYS to obtain the results. The appropriate analysis system used for this lab was fluid flow (Fluent). Under geometry properties, the analysis type was changed from 3D to 2D. It was assumed that the geometry file was given on Canvas, but it was of a rectangular shape with a length of 1219.2 mm and a height of 25.4 mm. The orifice plate is depicted as a short line halfway through the pipe (609.6 mm from the left), with a perpendicular length of 6.35 mm.

After finishing geometry, the next step was to generate the mesh. First, the type was changed from solid to fluid, and the methods were changed to triangles. Named edges were created with the following names: left edge as “Inlet,” right edge as “Outlet,” top edge as “PipeWall,” bottom edge as “Center line,” and center edge as “OrificePlate.”  $1e-4$  for the minimum size was then entered under sizing. For this lab, the maximum face size was the changing variable for the nine datasets, because it determined how fine the mesh was. For the coarse mesh  $1e-3$  was entered,  $8e-4$  was entered for the medium mesh, and  $5e-4$  for the fine. After this was done, generate mesh was hit. Under statistics, the number of nodes and elements were listed. These were only to change if the maximum face size was changed.

Next up was the physics settings. First, settings were changed to axisymmetric and it was confirmed that viscosity was set as laminar. Material was created to add “water-liquid (h<sub>2</sub>O)” from Fluent database, then under cell zone condition, set the new water-liquid as fluid. Under boundary condition type, the following types were changed: Inlet as velocity inlet, Interior-Fluid

as interior, OrificePlate as wall, Outlet as outflow, and PipeWall as wall. Additionally, under inlet, input the velocity magnitude solved from Equation [1]. Under solution monitors, the x, y, and continuity velocity absolute criteria to  $1e-4$  were changed, then initialize solution was pressed when computing from inlet. The calculation was run with 1000 iterations, and it was necessary to wait until the solution converged at some point between 1 and 1000. For computing drag on the OrificePlate, forces were selected under report, then the results were printed. The number under the printed “total” was the drag force.

Now, the lab is correctly set-up, and so the data sets could be obtained under results. For XY-plot of pressure along the centerline, the xy-plot button was selected, default settings were maintained, “Centerline” under surfaces was selected, and then save/plot was clicked. The corresponding plot then appeared on the screen. For velocity and pressure magnitude contours, the contour button was first selected, and the location to “periodic 1” was set. The variable was set to radial velocity (“velocity u”), and later after obtaining the results, the variable was changed to “pressure.” Applying the settings first to velocity, a variety of colors should appear on the pipe. To gain even more colors, the number of contours was changed from 11 to 51. To scale diagram, the “apply scale” was checked under view, and 10 was entered in the radial direction. To reflect the diagram, “apply reflection/mirroring” under view was checked, and the ZX plane under the method dropdown menu was selected. Apply these settings and uncheck wireframe for best image. For the velocity profile at the outlet plot, a line at the outlet was created. For point 1, “0.6096, 0, 0” for the coordinates in meters was entered into the prompt. For Point 2, “0.6096, 0.0254, 0” was entered. These are the coordinates for the outlet of the pipe. Select the char button, and then the data series tab. The location is set to the line made at the pipe outlet. Under the X-axis tab, the variable was changed to the axial velocity (“velocity u”). Under the Y-axis tab, the variable was changed to the radial distance (“Y”). The title name was changed and the settings were applied, then the plot appeared on the screen. Data was then exported to receive the data points on a sheet. After following these steps, enough data was gathered to analyze the results for all nine simulations.

## 4. Results

As mentioned previously, nine simulations were run. There were three Reynold’s Numbers that were tested (50, 100, and 150), and each corresponded to a laminar flow-speed and a flow rate less than 22 GPM. Each flow speed simulation was run using a coarse, medium, and fine mesh refinement. It was necessary to input the velocity corresponding to each Reynold’s Number, and a sample calculation for how these were found can be seen in Appendix C. The velocities for the Reynold’s Numbers of 50, 100, and 150 were  $8.76 \times 10^{-4} \frac{m}{s}$ ,  $17.52 \times 10^{-4} \frac{m}{s}$ , and  $26.28 \times 10^{-4} \frac{m}{s}$ , respectively.

For each of the nine simulations, the amount of nodes and elements in the mesh were also recorded. The residual plots were run using ANSYS, and once the output values for continuity, x-velocity, and y-velocity fell below an error of  $1 \times 10^{-4}$  the amount of iterations the simulation took to achieve this were recorded. The data for velocity, mesh refinement, nodes, elements, iterations until convergence, and the drag force measured can all be seen in Table A1.

Table A1.

Simulation Number	Velocity m/s	Reynolds	Mesh	Nodes	Elements	Convergence Iterations	Drag Force (N)
1	0.000876	50	coarse	32796	63101	577	9.68E-07
2	0.000876	50	medium	53018	102922	645	8.84E-07
3	0.000876	50	fine	122509	240038	816	9.82E-07
4	0.00175	100	coarse	32796	63101	685	3.05E-06
5	0.00175	100	medium	53018	102922	749	2.63E-06
6	0.00175	100	fine	122509	240038	939	2.89E-06
7	0.00263	150	coarse	32796	63101	813	6.26E-06
8	0.00263	150	medium	53018	102922	864	5.32E-06
9	0.00263	150	fine	122509	240038	985	5.85E-06

Once all of the data from above was gathered, there was a series of contour plots and graphs that were also produced from ANSYS. This included an axial velocity contour, an axial pressure contour, and an XY line-plot of pressure variation along the x-axis. One of each of these types of plots can be seen below and correlates to Simulation 3 (Reynolds Number=50 and a fine mesh refinement). Figure B1.3 gives the axial velocity contour, Figure B2.3 shows the axial pressure contour, and Figure B3.3 provides the XY line-plot of pressure variation. The remaining Figures can be seen in Appendix B as Figures B1.1 through B3.9.

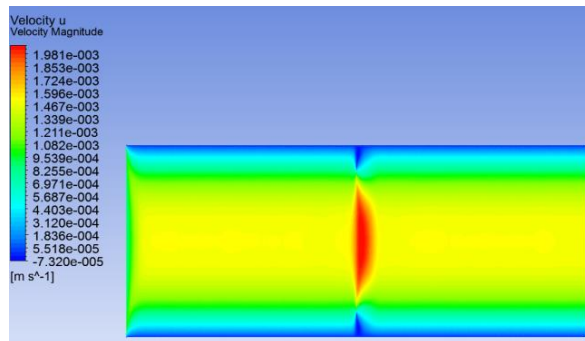


Figure B1.3.

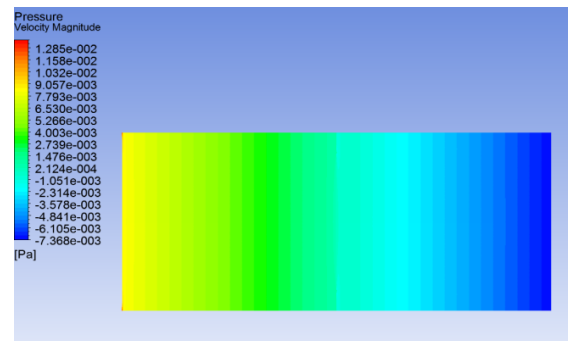


Figure B2.3.

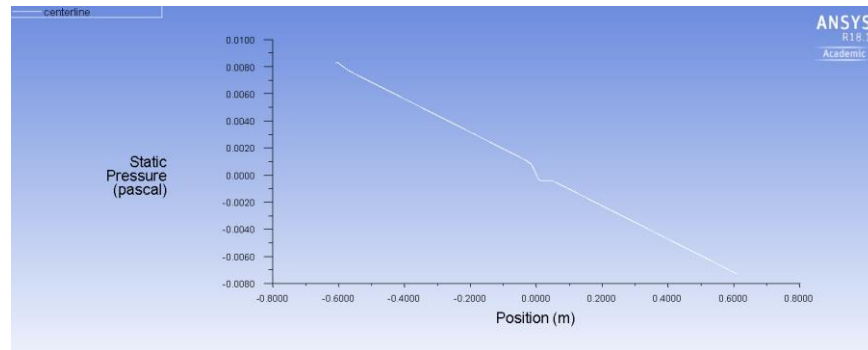


Figure B3.3.

Along with the above contours and plots, an axial velocity profile plot along the outlet was also produced for each of the three velocities that corresponded to a unique Reynolds Number. The three plots can be seen in Figures B4.1 through B4.3 in Appendix B, however, the one for a Reynolds Number of 50 (Velocity=.00089 m/s) can be seen below in Figure B4.1.

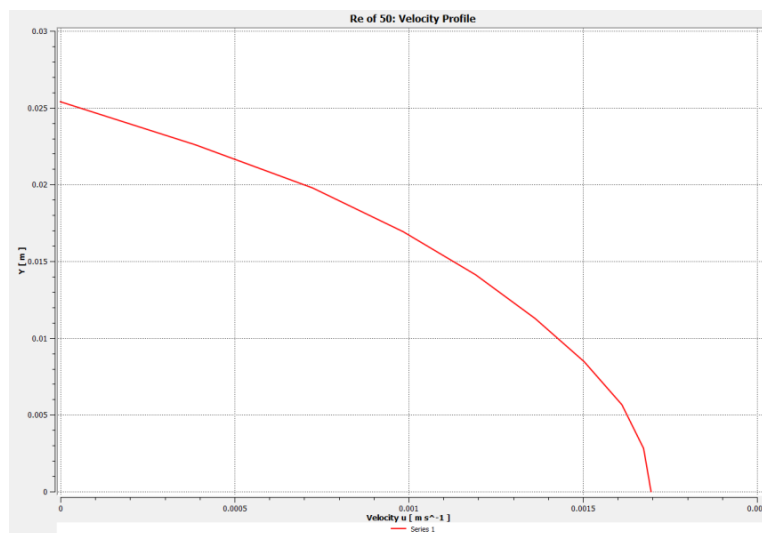


Figure B4.1

The last pieces of data that were collected and compiled into a graph were the drag forces on the orifice-plate for each of the nine simulations run. The line graph shown in Figure B5 provides the visual based on the amount of nodes that were recorded for each simulation test. The data was taken from Table A1.

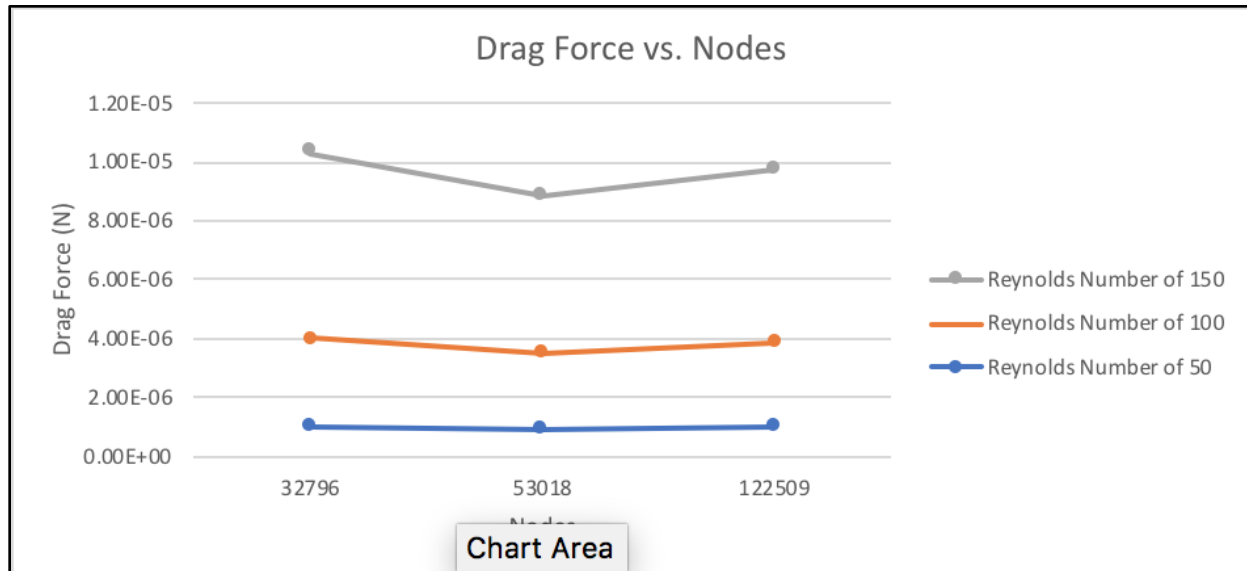


Figure B5.

Once all of the contours, plots, and tables were formed, they could then be analyzed for trends and how the mesh refinement changed the results.

## 5. Analysis and Discussion

The first part of the results that were analyzed were the velocity and pressure contour plots. The velocity contours can be seen in Figures B1.1 through B1.9, and show certain trends when only the mesh was changed and the Reynolds Number was kept constant. As seen for all nine plots, the velocity is the lowest on the outsides of the tube near the walls (indicated by the dark blue), and gets quicker the closer it gets to the center (shown by the yellows and oranges). While this trend was constant among all of the trials, there was a difference when the mesh refinement got smaller. When looking at the Reynolds Number of 50 plots, the velocities near the center of the tube were less continuous for the coarse refinement, and got more blended as the mesh became smaller. This can be seen as the patchy orange that occurred with the coarse and medium in Figures B1.1 and B1.2, and how there was almost a continuous and smooth contour for the fine mesh. Not only this, but the very high velocity contour that occurs directly between the obstructions takes a different shape as the mesh is changed. In Figure B1.1 where the mesh was coarse, the velocity was high between the obstructions, but created almost a bell shape as it moved along toward the right. As the mesh became more refined, this bell shaped appearance disappeared to the point that there was a thin red section directly in the center (high velocity) that was surrounded by the yellow instead of a fade from orange. This was the same trend that occurred for both the Reynolds Number of 100 and 150, as well.

The other piece of the velocity contours that can be compared are between certain Reynolds Numbers, and thus differing velocities. If the velocity contours of the fine mesh are compared across the Reynolds Numbers, it is found that the bell shape at the center is appears longer and

more drawn out for the larger Reynolds Number. This larger Reynolds Number leads to the higher velocity for these trials, and this creates more of the gradient in color seen on these plots. The obstruction produces more of an issue with the higher velocity simulations, as there must be a larger difference between the “zero” velocity at the tube walls and the narrow canal at the center. When the coarse and medium meshes are compared across the three varying Reynolds Numbers, they produce the same trend, that the bell is much larger and drawn out for the high values.

The next section of data collected was the pressure contour plots. These were also compared keeping the Reynolds Number constant, as well as between the three Reynolds Numbers. In the first case, the Reynolds Number of 50 can be taken into consideration to analyze the trend. This can be seen in Figures B2.1 through B2.3. The pressure for the coarse mesh starts off relatively high, which is indicated by the orange color at the inlet, and decreases smoothly until the color is a dark blue. As the mesh becomes more refined, the inlet pressure descriptor color becomes more yellow. This trend appeared across all three of the Reynolds Numbers. While it would be easy to say that as the mesh became more refined the inlet pressure decrease, this isn't as straightforward as it appears. The values that the colors indicate, which can be seen to the left of each contour, are not equal among all of the trials. The best use for these colors are to see the relative pressure differences across the tube. As the fluid moves along the tube to the right, the pressure decreased in all cases, becoming negative after the center, and more negative towards the outlet.

The contours can also be analyzed partially across the different Reynolds Numbers. While the meanings of the colors varies across the plots, the trend can still be seen. With the higher Reynolds Number of 150, the obstruction was more visible in the pressure contour plot. The negative pressure could be seen as two small vertical lines at the center of the tube where the obstructions to flow were located. This indicated that as the Reynolds Number increased, the velocity increased, and it caused the pressure to drop significantly near these obstructions. The finer the mesh was, the more prominent these low pressure areas became. This could be due to the fact that the more elements that were used in the calculation allowed the program to be more accurate in solving for what the true pressure was in these areas.

The XY line-plots for each of the nine trials can be seen in Figures B3.1 through B3.9. The overall trend of these plots show that as the position moves to the right in the x direction, the pressure decreased. All nine of the plots have a negative linear relationship, with the exception of what happens at  $x=0$ . This is where the obstruction is located, and causes a more drastic and abrupt decrease then increase in the pressure. For all three of the cases using the Reynolds Number of 50, the plots were nearly identical, where the pressure at the inlet is close to .008 Pa and drops to -.008 Pa at the outlet. This occurred again with the Reynolds Number of 100 where the inlet pressure was .0175 Pa and dropped to -.0125 at the outlet, and with the Reynolds Number of 150 where it started at .0275 Pa and exited at -.0175 Pa. While the overall trend between the plots remained the same, the severity of the dip at  $x=0$  changed with the differing Reynolds Numbers. As the Reynolds Number increased, the depth of the jump also increased, where it was largest with the Reynolds number of 150. This also agrees with the contour plots mentioned previously, as with these three trials, the negative pressure was visible at the obstruction by the dark blue colors on the contours.



The outlet velocity profiles were also analyzed and can be seen in Figures B4.1 through B4.3. This plot was only dependent on the Reynolds Number and not the mesh refinement, thus there were only three distinct plots. Each describes the axial velocity at the outlet across the Y position, and has the same shape. Due to the fact that the diameter did not change between simulations, the y-axis was the same for each plot. The x-axis did change; however, because the Reynolds number impacted the inlet velocity, which impacted the outlet velocity. The slope of each plot got steeper and steeper, which indicated that as the y position got closer to the center, the axial velocity was increasing at a quicker rate. This coincides with the velocity contours discussed previously. The Reynolds Number that produced the highest outlet velocities along the vertical direction was 150, the middle was 100, and the lowest was 50. This makes sense, as the velocity entered into the program that corresponded to these Reynolds number follow the same trend.

Lastly, the mesh convergence plot for each of the three flow speeds was looked at. The plot consisted of the drag force on the orifice-plate that corresponded to the amount of nodes and each Reynolds Number. This can be seen in Figure B5. Due to the fact that all of the coarse, medium, and fine meshes had the same amount of nodes, the plots for each of the Reynolds Numbers are stacked. It can be seen that the overall trend for each of the lines was that the smallest number of nodes (coarse mesh) had the highest drag force, the middle amount of nodes (medium mesh) had the smallest, and the largest amount of nodes (fine mesh) had slightly higher. When looked at on the graph, the values all fall extremely close together, with the middle only dipping slightly. This is especially true for the Reynolds Number of 50, where the line appears almost horizontal. This is expected, as after a certain number of nodes the outputs, such as drag force, are no longer dependent on the mesh. Due to the fact that the plots are close to even, it was assumed that drag force had already hit this constant value with the mesh refinements tested. If more tests were to be done in the future, both higher and lower refinements would be tested to create more points and see where this constant value occurred. While it was odd that the medium mesh produced a lower drag force, these simulations were tested again and gave the same results. Also, the fact that it was a minimal drop when compared to the other surrounding values allowed for the assumption that it was due to the fact that once the mesh hit a certain size the drag force would be 100% identical for all meshes beyond that point.

As mentioned previously, the number of iterations that each simulation took to converge was recorded. This value is the number of times the computer ran the numbers to get the results within a certain error of the answer. These values can be seen in Table A1 for each of the simulations. The maximum number of iterations that were run for each test was 1000, and the computer would have output that it could not converge if this were too few. In the case of this lab, all combinations of Reynolds Number and mesh size converged, and there was a trend in the amount of iterations required for this. Across a specific Reynolds Number, the coarse mesh took the fewest iteration, the medium the next largest, and the fine mesh the most iterations. For the case of the Reynolds Number of 50, the coarse mesh took 577, the medium 645, and the fine 816. This was the same for the Reynolds Number of 100 where it was 685 for coarse, 749 for medium, and 939 for the fine, as well as for the Reynolds Number of 150 where it was 813, 864, and 985. This occurs because the finer the mesh is, the more elements that the geometry is broken into. The program must run the calculations across each of the elements, which takes longer for the larger amount of elements and nodes. What can also be seen by the convergence numbers mentioned above is that

the higher the Reynolds Number, the more iterations that were necessary for the calculations to be within the specified error.

Because this lab was run using CFD, there were fewer spots for error to occur. The accuracy of the results is set by the desired error for the simulation to be run in, but all the calculations were left up to the computer. While this was true, there were always places of error where conditions were being entered for each simulation. This could have caused variance in some of the values, but in order to decrease this chance the inputs were always double checked.

## **6. Summary and Conclusion**

The objective of this lab was to determine if output solutions by ANSYS are dependent on the mesh refinement chosen, while simultaneously investigating the differences in velocity and pressure distributions caused by an obstruction at different flow rates. Nine simulations on ANSYS, a computational fluid dynamics program, were run that consisted of combinations of a coarse, medium, and fine mesh refinements, as well as a Reynolds Number of either 50, 100, and 150. Using the drag force on the orifice-plate as the output variable, it was found that there was a point at which the amount of elements the domain was divided into was unimportant. For all three unique Reynolds Numbers the graph of drag force vs. elements were extremely close to horizontal, leading to the conclusion that there was a point at which the mesh refinement made no difference on the output solution. The medium mesh refinement produced a slightly lower output than the coarse and fine meshes, but this was attributed to the fact that it was highly unlikely the output be completely equal in all cases. The amount of elements chosen was not a large enough range to find the point at which the mesh size was insignificant, as all cases produced similar values. In future cases, a wider range of mesh sizes would be tested, to better understand the amount of elements that was fine enough for the output to not rely on. The three Reynolds Numbers were used to calculate the input speeds, where the largest velocity came from the Reynolds Number of 150, and it decreased from there. It was found that the larger the flow rate, the more of an impact the obstruction made. For the highest velocity the obstruction appeared darker in color on the pressure contours, which meant that there was negative pressure along where those were located in the domain. The velocity contours had a larger bell-shaped appearance past the obstruction, meaning that the velocity was at a higher speed for longer once that point was passed. This was thought to occur due to the fact that the fluid had to move faster for a longer period of time, because there was a larger velocity difference between the outer walls and the center for higher speed fluid. Overall, it was discovered that there was a certain number of elements in the mesh that caused the outputs to be almost equal, however, it would be better to run more simulations in the future to better see where this point was. It was also found that the velocity and pressure at certain points within the tube were dependent on the flow rate that was input into the program.

## 7. References

[1] *Intro CFD Powerpoint Presentation*. Iowa State Mechanical Engineering Department, 2017.

[2] *LAB 5: CFD (Orifice Plate)*, Iowa State Mechanical Engineering Department, 2017.

## 8. Appendix

### Appendix A

Table A1: Data taken from ANSYS for each simulation.

Simulation Number	Velocity m/s	Reynolds	Mesh	Nodes	Elements	Convergence Iterations	Drag Force (N)
1	0.000876	50	coarse	32796	63101	577	9.68E-07
2	0.000876	50	medium	53018	102922	645	8.84E-07
3	0.000876	50	fine	122509	240038	816	9.82E-07
4	0.00175	100	coarse	32796	63101	685	3.05E-06
5	0.00175	100	medium	53018	102922	749	2.63E-06
6	0.00175	100	fine	122509	240038	939	2.89E-06
7	0.00263	150	coarse	32796	63101	813	6.26E-06
8	0.00263	150	medium	53018	102922	864	5.32E-06
9	0.00263	150	fine	122509	240038	985	5.85E-06

### Appendix B

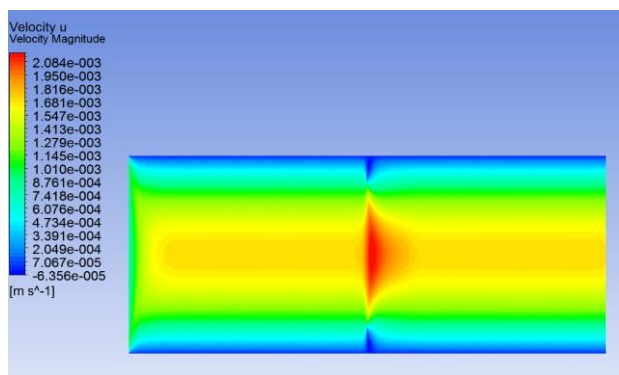


Figure B1.1: Provides the ANSYS axial velocity contour for a Reynolds Number of 50 and a Coarse mesh refinement.

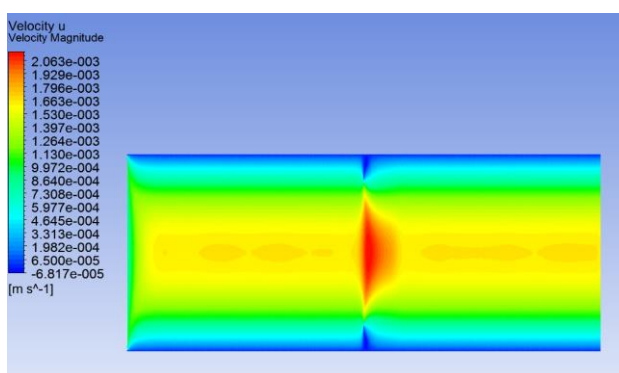


Figure B1.2: Provides the ANSYS axial velocity contour for a Reynolds Number of 50 and a Medium mesh refinement.

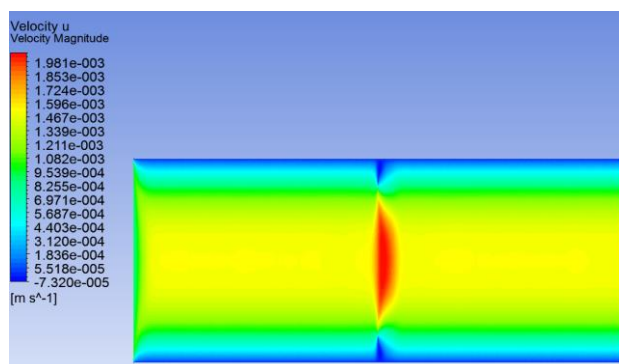


Figure B1.3: Provides the ANSYS axial velocity contour for a Reynolds Number of 50 and a Fine mesh refinement.

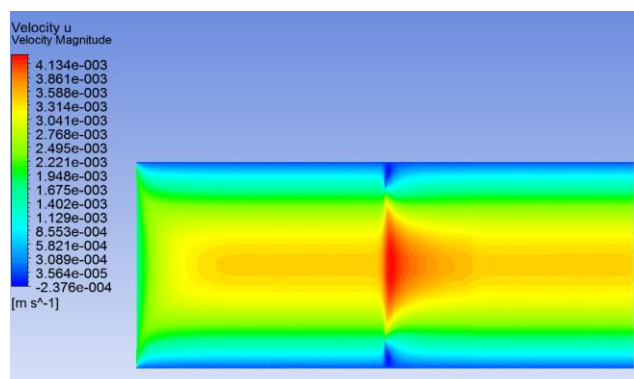


Figure B1.4: Provides the ANSYS axial velocity contour for a Reynolds Number of 100 and a Coarse mesh refinement.

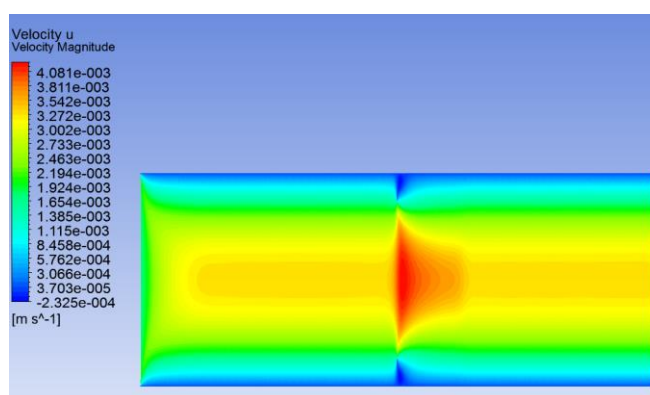


Figure B1.5: Provides the ANSYS axial velocity contour for a Reynolds Number of 100 and a Medium mesh refinement.

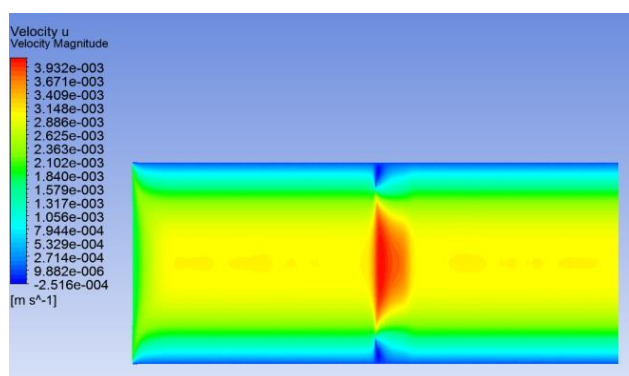


Figure B1.6: Provides the ANSYS axial velocity contour for a Reynolds Number of 100 and a Fine mesh refinement.

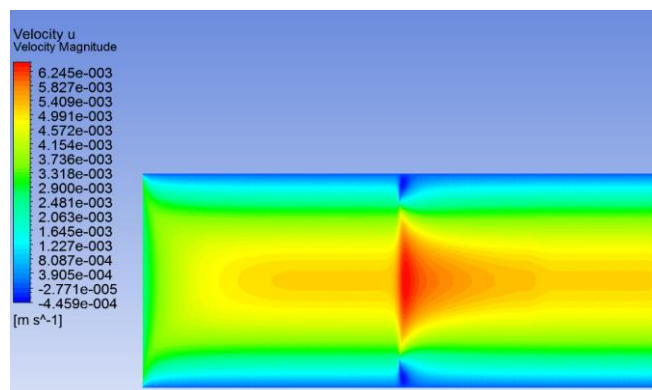


Figure B1.7: Provides the ANSYS axial velocity contour for a Reynolds Number of 150 and a Coarse mesh refinement.

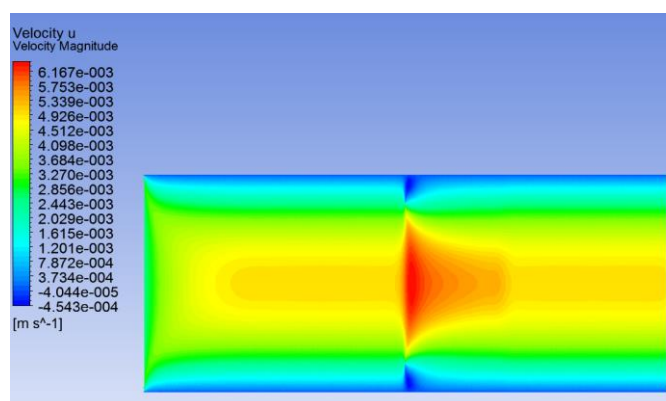


Figure B1.8: Provides the ANSYS axial velocity contour for a Reynolds Number of 150 and a Medium mesh refinement.

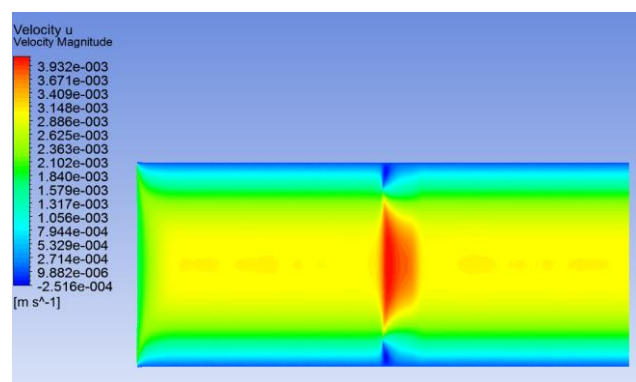


Figure B1.9: Provides the ANSYS axial velocity contour for a Reynolds Number of 150 and a Fine mesh refinement.

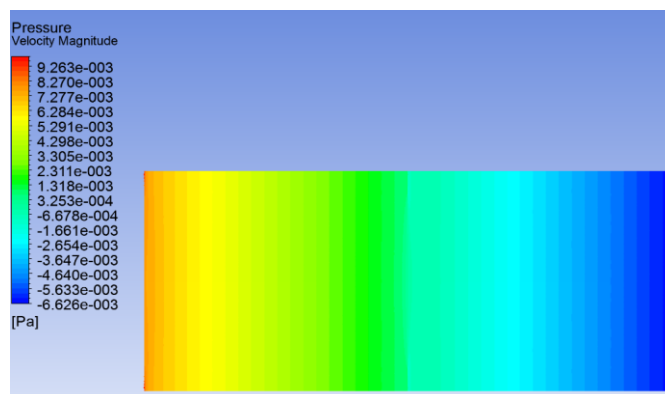


Figure B2.1: Gives the ANSYS axial pressure contour for a Reynolds Number of 50 and a Coarse mesh refinement.

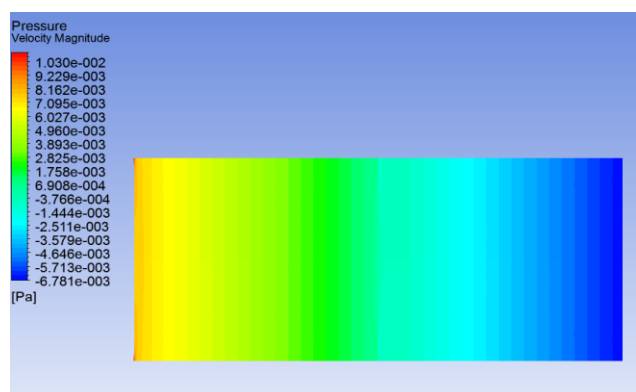


Figure B2.2: Gives the ANSYS axial pressure contour for a Reynolds Number of 50 and a Medium mesh refinement.

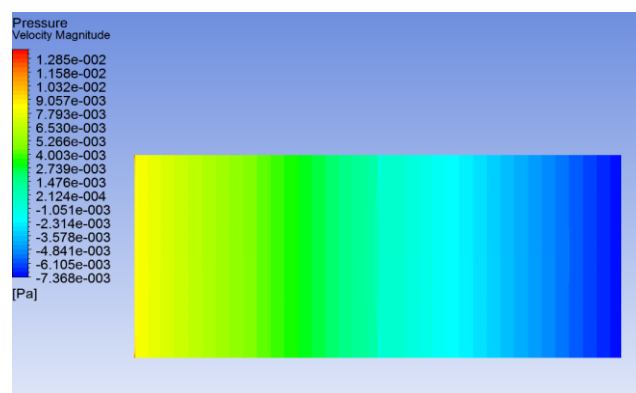


Figure B2.3: Gives the ANSYS axial pressure contour for a Reynolds Number of 50 and a Fine mesh refinement.

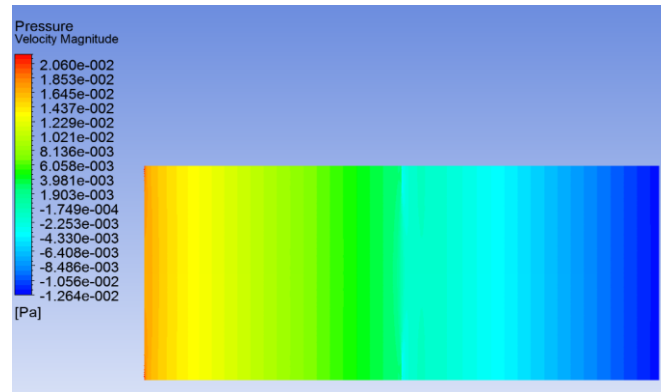


Figure B2.4: Gives the ANSYS axial pressure contour for a Reynolds Number of 100 and a Coarse mesh refinement.

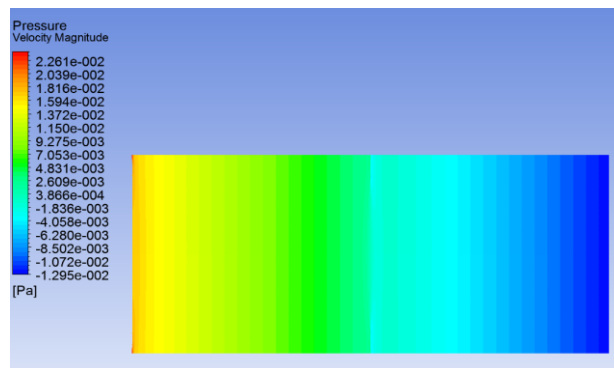


Figure B2.5: Gives the ANSYS axial pressure contour for a Reynolds Number of 100 and a Medium mesh refinement.

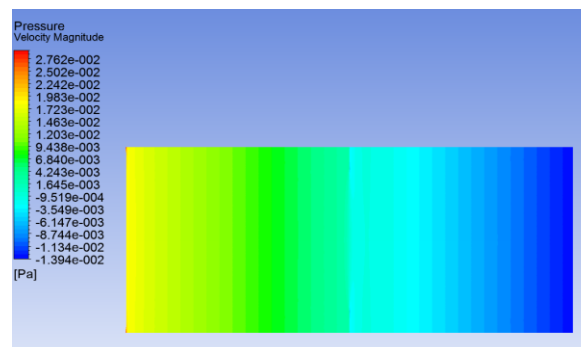


Figure B2.6: Gives the ANSYS axial pressure contour for a Reynolds Number of 100 and a Fine mesh refinement.



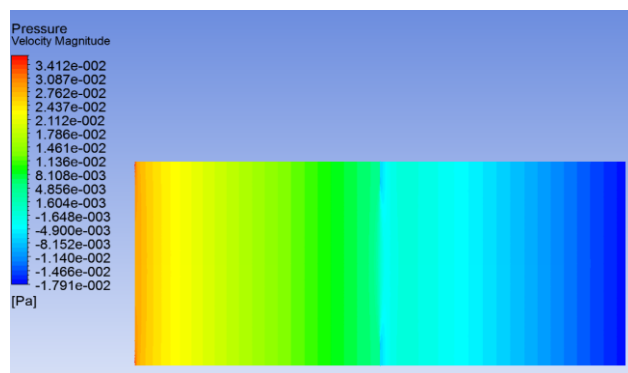


Figure B2.7: Gives the ANSYS axial pressure contour for a Reynolds Number of 150 and a Coarse mesh refinement.

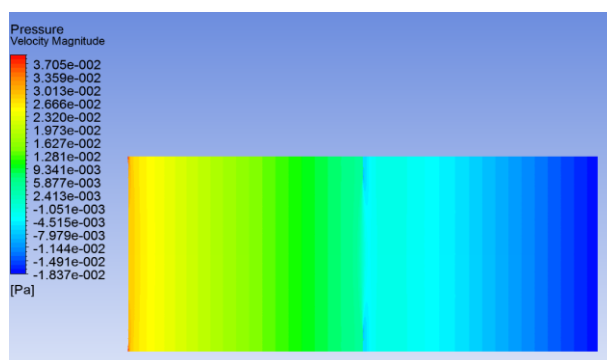


Figure B2.8: Gives the ANSYS axial pressure contour for a Reynolds Number of 150 and a Medium mesh refinement.

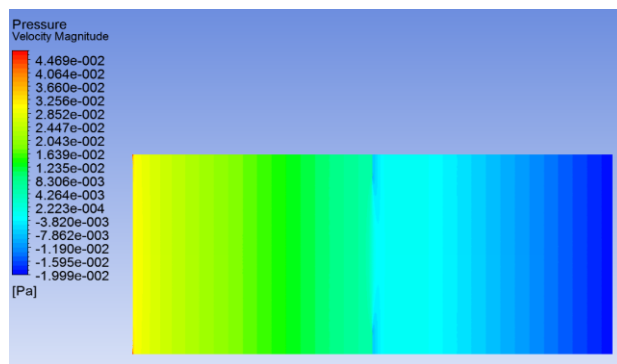


Figure B2.9: Gives the ANSYS axial pressure contour for a Reynolds Number of 150 and a Fine mesh refinement.

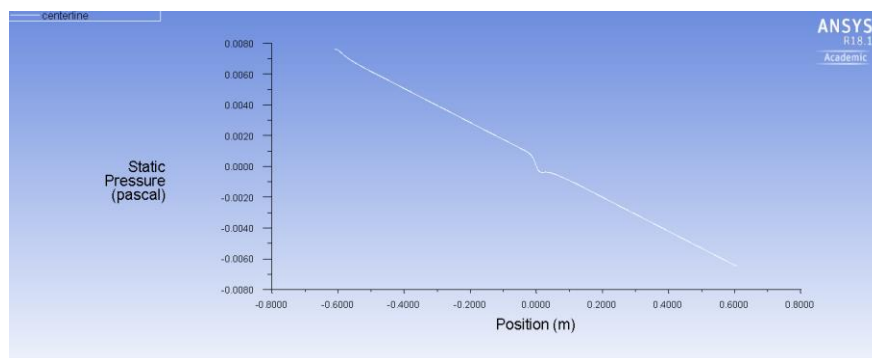


Figure B3.1: Depicts the ANSYS XY line-plot of pressure variation along the axial direction for a Reynolds Number of 50 and a Coarse mesh refinement.

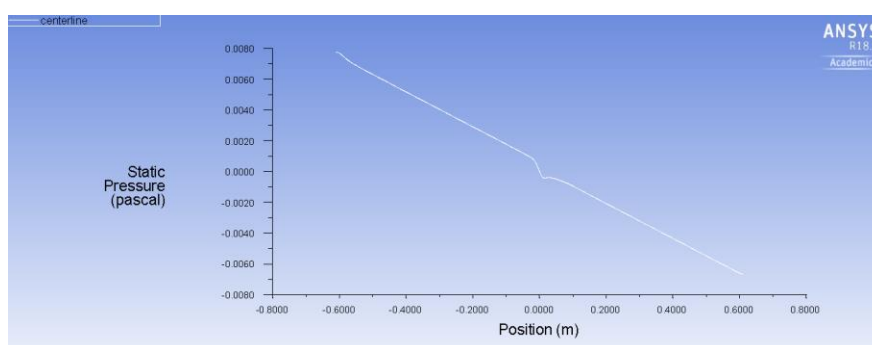


Figure B3.2: Depicts the ANSYS XY line-plot of pressure variation along the axial direction for a Reynolds Number of 50 and a Medium mesh refinement.

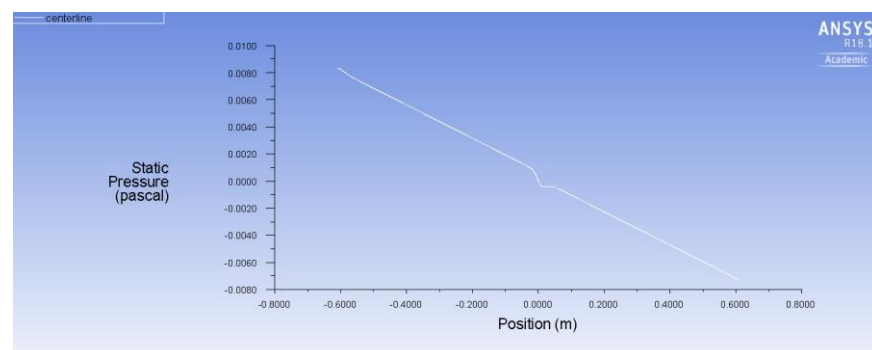


Figure B3.3: Depicts the ANSYS XY line-plot of pressure variation along the axial direction for a Reynolds Number of 50 and a Fine mesh refinement.

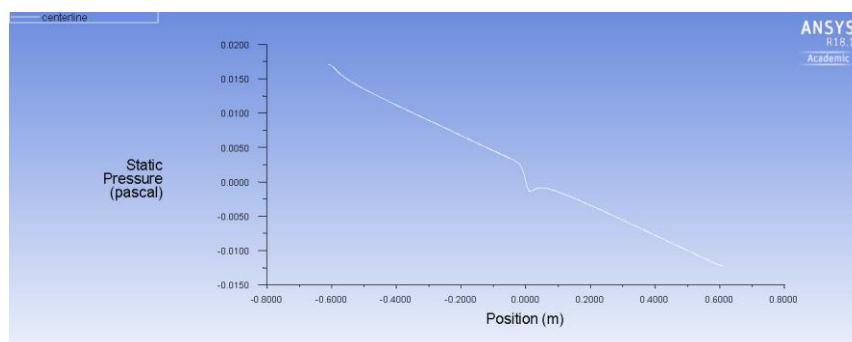


Figure B3.4: Depicts the ANSYS XY line-plot of pressure variation along the axial direction for a Reynolds Number of 100 and a Coarse mesh refinement.

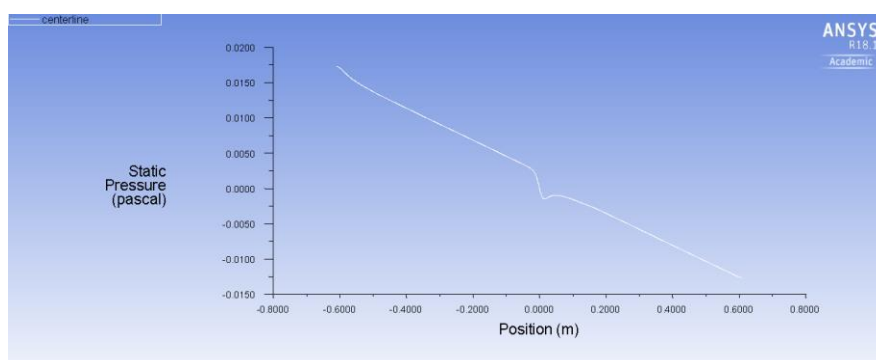


Figure B3.5: Depicts the ANSYS XY line-plot of pressure variation along the axial direction for a Reynolds Number of 100 and a Medium mesh refinement.

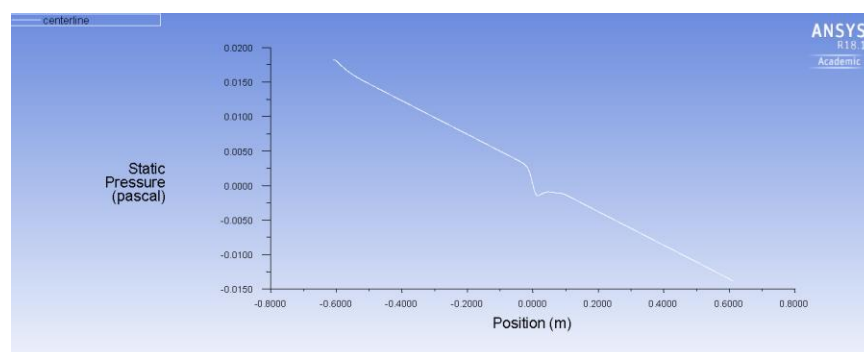


Figure B3.6: Depicts the ANSYS XY line-plot of pressure variation along the axial direction for a Reynolds Number of 100 and a Fine mesh refinement.

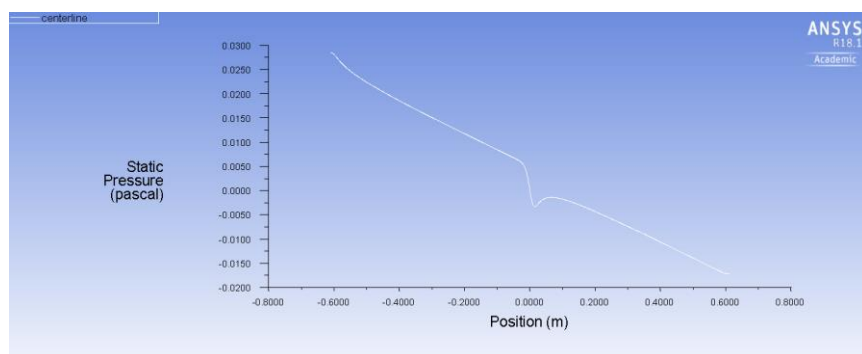


Figure B3.7: Depicts the ANSYS XY line-plot of pressure variation along the axial direction for a Reynolds Number of 150 and a Coarse mesh refinement.

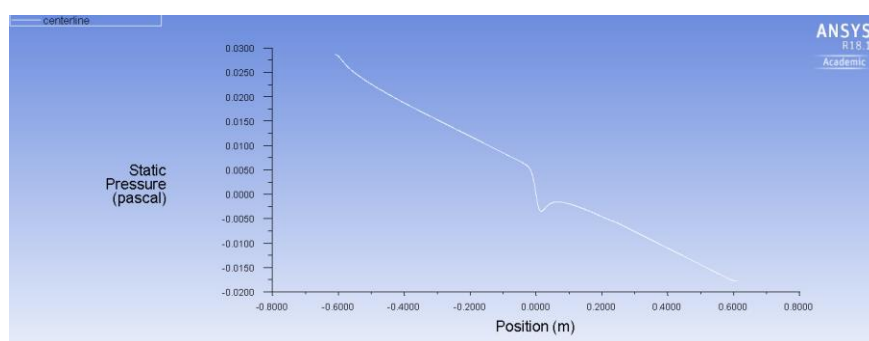


Figure B3.8: Depicts the ANSYS XY line-plot of pressure variation along the axial direction for a Reynolds Number of 150 and a Medium mesh refinement.

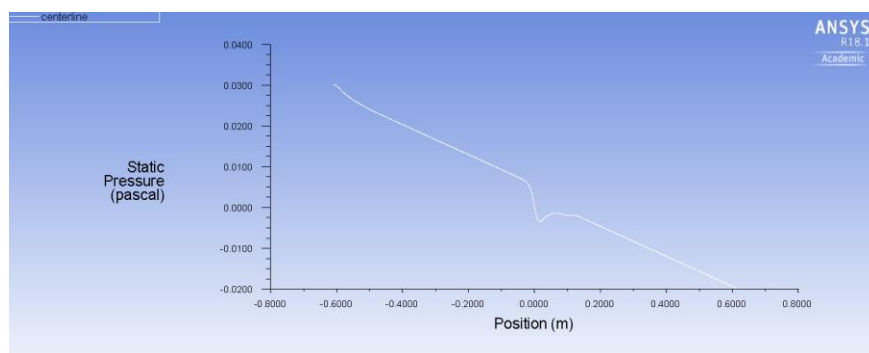


Figure B3.9: Depicts the ANSYS XY line-plot of pressure variation along the axial direction for a Reynolds Number of 150 and a Fine mesh refinement.

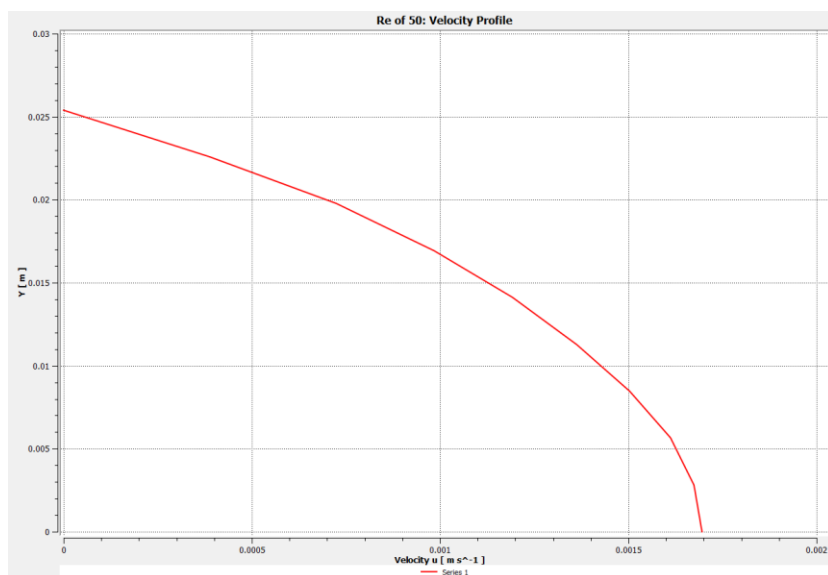


Figure B4.1: Outlet axial velocity profile at given Y values for a Reynolds Number of 50.

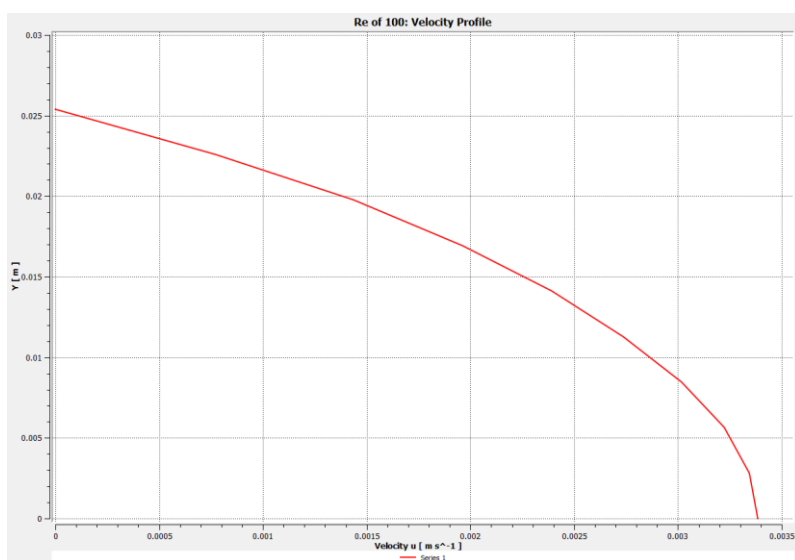


Figure B4.1: Outlet axial velocity profile at given Y values for a Reynolds Number of 100.

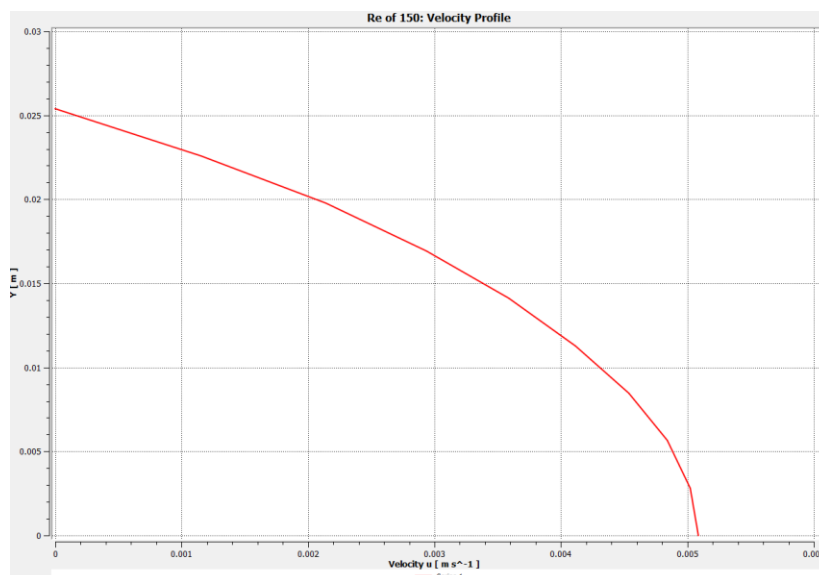


Figure B4.1: Outlet axial velocity profile at given Y values for a Reynolds Number of 150.

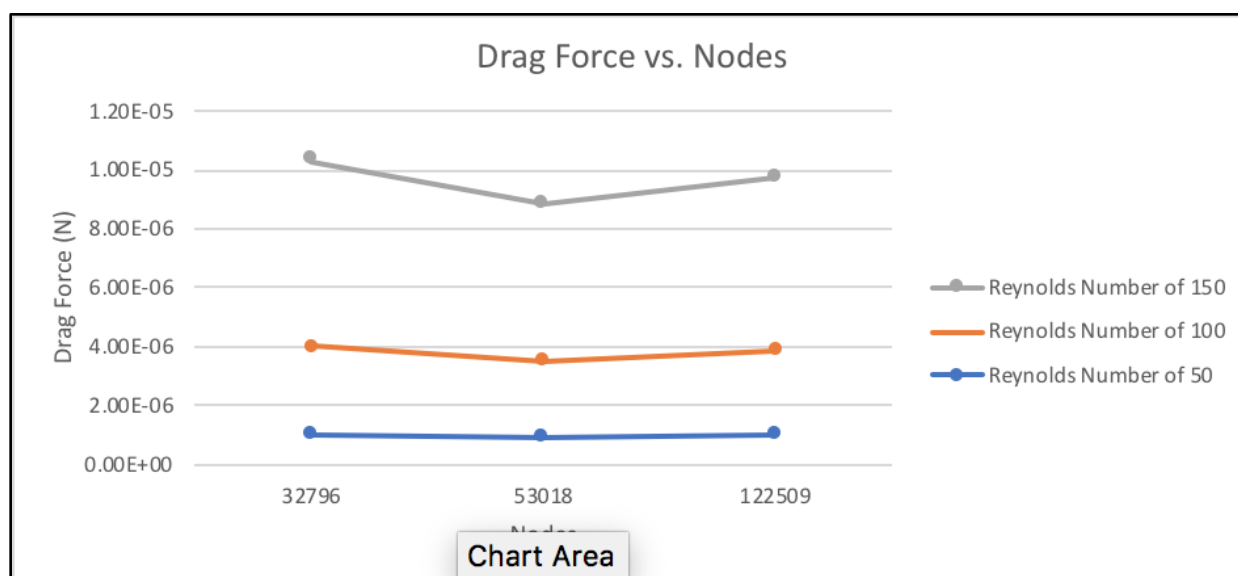


Figure B5: Combined plot of three different Reynolds Numbers of the drag force on the orifice plate for each amount of nodes, which correspond to the coarse, medium, and fine meshes.

### Appendix C

In order to determine the velocity corresponding to each Reynolds Number, the equation for Reynolds Number (Re) was used. This is given by the dimensionless ratio of inertial forces to viscous forces, and quantifies the viscous effects. It can be found by taking the product of the fluid's density ( $\rho$ ), the characteristic velocity ( $v$ ), and the characteristic length ( $D$ ), all divided by the absolute viscosity ( $\mu$ ). This can be seen in Equation 1.

$$Re = \frac{\rho v D}{\mu} \quad \text{Equation [1]}$$

Sample Calculation for the velocity of the fluid using a Reynolds Number of 50 and Equation 1.

$$Re = 50 \quad \rho = 1000 \frac{kg}{m^3} \quad D = 2 \text{ in} = .0508 \text{ m} \quad \mu = .00089 \frac{Ns}{m^2}$$

$$Re = \frac{\rho v D}{\mu} \quad v = \frac{Re(\mu)}{\rho D} = \frac{50(.00089)}{1000(.0508)} = 8.76 \times 10^{-4} \frac{m}{s}$$